On a coherent investigation of the spectrum of cosmic rays in the energy range of 10^{14} – 10^{18} eV with KASCADE and KASCADE-Grande

Journal of Physics: Conference Series **632** (2015) 012025 doi:10.1088/1742-6596/632/1/012025

On a coherent investigation of the spectrum of cosmic rays in the energy range of 10^{14} - 10^{18} eV with KASCADE and KASCADE-Grande

S Schoo[1], W D Apel[1], J C Arteaga-Velázquez[2], K Beck[1], M Bertaina[3], J Blümer[1,4], H Bozdog[1], I M Brancus[5], E Cantoni[3,6,a], A Chiavassa[3], F Cossavella[4,b], K Daumiller[1], V de Souza[7], F Di Pierro[3], P Doll[1], R Engel[1], D Fuhrmann[8,c], A Gherghel-Lascu[5], H J Gils[1], R Glasstetter[8], C Grupen[9], A Haungs[1], D Heck[1], J R Hörandel[10], D Huber[4], T Huege[1], K H Kampert[8], D Kang[4], H O Klages[1], K Link[4], P Łuczak[11], H J Mathes[1], H J Mayer[1], J Milke[1], B Mitrica[5], C Morello[6], J Oehlschläger[1], S Ostapchenko[12], N Palmieri[4], M Petcu[5], T Pierog[1], H Rebel[1], M Roth[1], H Schieler[1], F G Schröder[1], O Sima[13], G Toma[5], G C Trinchero[6], H Ulrich[1], A Weindl[1], J Wochele[1], J Zabierowski[11]

[1] Institut für Kernphysik, KIT - Karlsruher Institut für Technologie, Germany
[2] Universidad Michoacana, Instituto de Física y Matemáticas, Morelia, Mexico
[3] Dipartimento di Fisica, Università degli Studi di Torino, Italy
[4] Institut für Experimentelle Kernphysik, KIT - Karlsruher Institut für Technologie, Germany
[5] Horia Hulubei National Institute of Physics and Nuclear Engineering, Bucharest, Romania
[6] Osservatorio Astrofisico di Torino, INAF Torino, Italy
[7] Universidade São Paulo, Instituto de Física de São Carlos, Brasil
[8] Fachbereich Physik, Universität Wuppertal, Germany
[9] Department of Physics, Siegen University, Germany
[10] Dept. of Astrophysics, Radboud University Nijmegen, The Netherlands
[11] National Centre for Nuclear Research, Department of Astrophysics, Lodz, Poland
[12] Frankfurt Institute for Advanced Studies (FIAS), Frankfurt am Main, Germany
[13] Department of Physics, University of Bucharest, Bucharest, Romania
[a] now at: Istituto Nazionale di Ricerca Metrologia, INRIM, Torino
[b] now at: DLR Oberpfaffenhofen, Germany
[c] now at: University of Duisburg-Essen, Duisburg, Germany

E-mail: sven.schoo@kit.edu

Abstract. The KASCADE experiment and its extension KASCADE-Grande have significantly contributed to the current knowledge about the energy spectrum and composition of cosmic rays (CRs) with energies between the knee and the ankle. However, the data of both experiments were analysed separately, although Grande used the muon information of the KASCADE-array. A coherent analysis based on the combined data of both arrays is expected to profit from reconstructed shower observables with even higher accuracy compared to the stand-alone analyses. In addition, a significantly larger fiducial area is available.

The aim of this analysis is to obtain the spectrum and composition of CRs in the range from 10^{14} to 10^{18} eV with a larger number of events and further reduced uncertainties using one unique reconstruction procedure for the entire energy range. This contribution will describe the motivation, the concept, and the current status of the combined analysis.

1. Introduction

Up to now the measurements of the KASCADE/-Grande ([1],[2]) arrays have been analyzed independently of each other, though the KASCADE-Grande analyses used the shielded scintillation detectors of the KASCADE array for the reconstruction of the total number of muons (N_μ). There are several good reasons for combining the measurements of both arrays prior to the reconstruction of the shower observables. One is the expected increase in accuracy of the reconstructed shower sizes due to the additional information from the respective other detector setup and the increased distance range for the lateral distribution of charged particles ($N_{\rm ch}$). Another reason is, that a combined analysis should remove most of the differences in absolute flux observed between the KASCADE and KASCADE-Grande all-particle spectra and should result in one consistent composition measurement over the whole, combined energy range from around $10^{15} - 10^{18}$ eV and possibly even down towards 10^{14} eV. The layout of the KASCADE array and an outline of its stand-alone reconstruction of shower observables and energy will be shown in Section 2. The same information will be given for KASCADE-Grande in Section 3. Before presenting a short conclusion (Sec. 5) at the end of this article, the current status of the combined analysis will be given in Section 4.

2. KASCADE

2.1. The Experiment

The KASCADE experiment was located in Karlsruhe (Lon.: 8.4°, Lat.: 49.1°), Germany at an altitude of approximately 110 m a.s.l. The layout of the experiment with the array, the muon tracking detector and the central detector is shown on the left side of Fig. 1. The array consisted of 252 stations organized in 16 clusters. While the 192 stations of the outer 12 clusters were equipped with shielded and non-shielded scintillation detectors, the stations in the inner four clusters were built without the shielded scintillators, but with twice the number of e/γ detectors. As described in the next subsection, using this setup, the simultaneous reconstruction of $N_{\rm e}$ and N_μ is possible.

2.2. The Shower-Reconstruction

As a first step of the reconstruction the center of gravity of the signals of the non-shielded scintillation detectors (e/γ detector) is used to get a first estimate of the position of the core of the shower. The direction of the shower axis is estimated using a plane shower front. After weighting the signals of the e/γ and muon detectors with geometrical weights, the sum of these weighted deposits is used as the starting values for $N_{\rm e}$ and N_μ.

In a second step the arrival direction is improved by fitting a conically shaped shower front to the arrival times measured with the e/γ detectors. The core position, $N_{\rm e}$ and the shower-age are obtained by fitting a NKG-like lateral density function (LDF) [4][5] to the particle densities measured at the e/γ detectors. Prior to that, the energy deposits have been transformed into particle densities using a lateral energy correction function (LECF). The LECF describes the average energy deposited by a single charged particle depending on the distance of the station to the shower core and the size of the shower. The LECF used for the electromagnetic component is shown in Fig. 1 for three different shower sizes. The number of particles is calculated by dividing the total energy deposit by the effective energy deposited per single charged particle ($f_{\rm LECF}$) taking into account also the energy deposited by photons and the e/γ ratio. The shape of the LECF is explained in detail in [3].

At this stage the result of the fit corresponds to the number of charged particles at observation level since the energy deposited by muons has not been subtracted at this point.

The reconstruction of the number of muons is done simultaneously, therefore, in the third and last step the muon LDF is known and this information is included in the fitting procedure for the e/γ detectors resulting in the reconstruction of $N_{\rm e}$.

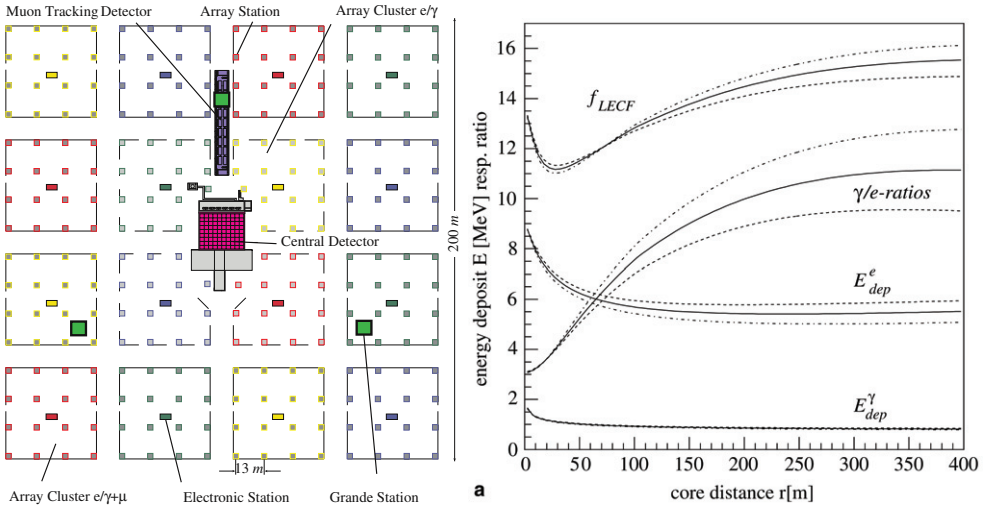

Figure 1. The layout of the KASCADE experiment is shown in the left picture. Each station was equipped with shielded and non-shielded scintillators, except for the stations of the inner four clusters, which were installed without the shielded scintillators (See [1]). In the right plot, the energy deposits per electron ($E^{\mathrm{e}}_{\mathrm{dep}}$) and γ ($E^{\gamma}_{\mathrm{dep}}$) are shown together with the γ/e ratio and the effective deposit per charged particle (f_{LECF}) for proton primaries and $\log_{10}N_{\mathrm{e}} = 5$ (dashed lines), $\log_{10}N_{\mathrm{e}} = 6$ (solid lines), $\log_{10}N_{\mathrm{e}} = 7$ (dotted dashed lines)(See [3]).

The reconstruction of the number of muons is very similar to the one for the number of electrons. The transformation of energy deposits to particle densities takes into account the N_{e}-dependent probability of electrons, photons or hadrons passing the shielding especially near the shower core. Since this faked muon deposit gets dominant below a distance of 40 m, stations within this distance to the shower core are excluded from the analysis. Further more, the NKG-like LDF is known to deviate from the true lateral muon distribution towards large core distances, therefore, the muon LDF is integrated only in the range from $40 - 200$ m, where the KASCADE detectors provide sampling points for the fit. The result is the truncated number of muons ($N^{\mathrm{tr.}}_{\mu}$). Because of the low muon densities, the shape parameter is fixed to a value derived using simulated showers taking into account also the dependence on the shower size. The only remaining free parameter is therefore the number of muons itself.

For a more detailed description of the reconstruction procedure see [3].

2.3. The Energy Spectrum

The reconstruction of the energy spectra for all particles together and separately for five masses is based on the two-dimensional shower-size spectrum shown in Fig. 2. In principle, every nucleus with a certain mass and energy should contribute only to specific cells depending on the intrinsic shower-to-shower fluctuations. The extent of these fluctuations depends on the mass and energy of the primary particle. The 'naturally' available region in the two-dimensional spectrum gets smeared out further by inaccuracies in the reconstruction of N_{e} and N_{μ} and the trigger- and reconstruction probabilities for showers of a certain size.

The problem can be expressed as

$$\vec{Y} = \mathbf{R}\vec{X} \tag{1}$$

with $\vec{Y}$ containing the cell contents in Fig. 2, $\vec{X}$ being the corresponding mass and energy and $\mathbf{R}$ being the *response matrix*. The unfolding technique used to solve this equation is described in [6], the resulting spectra for all particles, protons and helium using QGSJet01 [7] as the

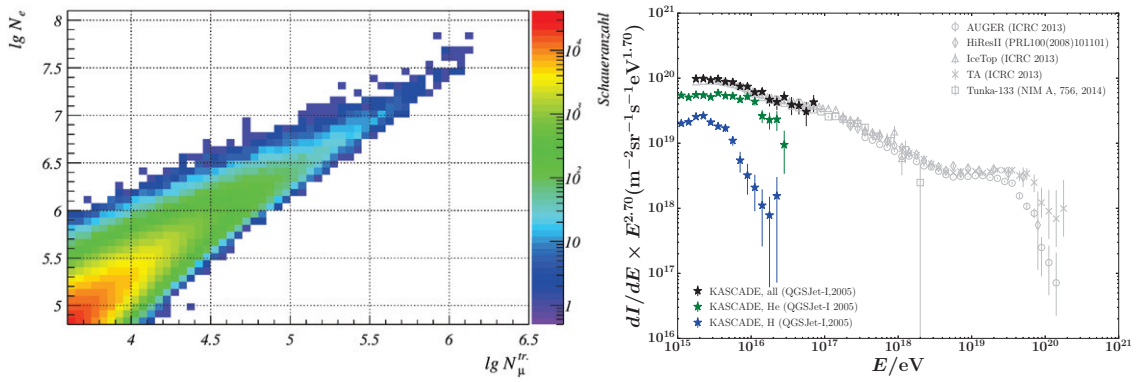

Figure 2. Left: The tow-dimensional shower-size spectrum measured with KASCADE. (See [6]); Right: The resulting, unfolded spectra for proton and helium together with the all-particle spectrum for the same analysis and other experiments.

hadronic interaction model are shown in Fig. 2. For a comparison with the results using the hadronic interaction model SIBYLL [8] and for the unfolded spectra for carbon, silicon and iron primaries, see Ref. [6].

An interesting discovery was that the knee-like structure at around 6 PeV in the all-particle spectrum might be caused primarily by a knee-like structure in the flux of helium instead of protons. However, one should not forget the dependence on the hadronic interaction model used in the simulations. A model that predicts much more muons, for example, would result in a significantly lighter composition. If the "proton-knee" is indeed located at an energy of around $2-3$ PeV, the helium knee would be expected to be at around $4-6$ PeV (in case of a charge dependence) or around $8-12$ PeV (in case of a mass dependence). Unfortunately the helium spectrum does not allow to distinguish between these two scenarios.

For iron primaries, the knee is expected to be just below 100 PeV (in case of a charge dependence), which is the upper limit of the energy range accessible with KASCADE. Its extension, KASCADE-Grande is capable of reconstructing events with energies up to 1 EeV and will be discussed in the next section.

3. KASCADE-Grande

KASCADE-Grande was located next to the KASCADE array with an overlap as it is shown in Fig. 3. Covering an energy range from 10 PeV up to 1 EeV, there is also an overlap between the energy spectra of both arrays.

The KASCADE-Grande stations were equipped with non-shielded scintillation detectors ($10\,\mathrm{m}^2$ per station) only, therefore, the reconstruction of the number of muons is only possible using the shielded detectors of the KASCADE array. The reconstruction procedure is explained in the next subsection.

3.1. The Shower-Reconstruction

The reconstruction of the shower-observables is again split into several steps. These steps will be briefly summarized in this section. A detailed description can be found in [2].

The first step is identical to the first step of the KASCADE reconstruction resulting in an estimate for the core position, arrival direction, number of charged particles (N_{ch}) and muons.

The LDF used for the electromagnetic component is again a modified NKG-function. The reconstruction of the number of muons, however, is based on a function described by Lagutin

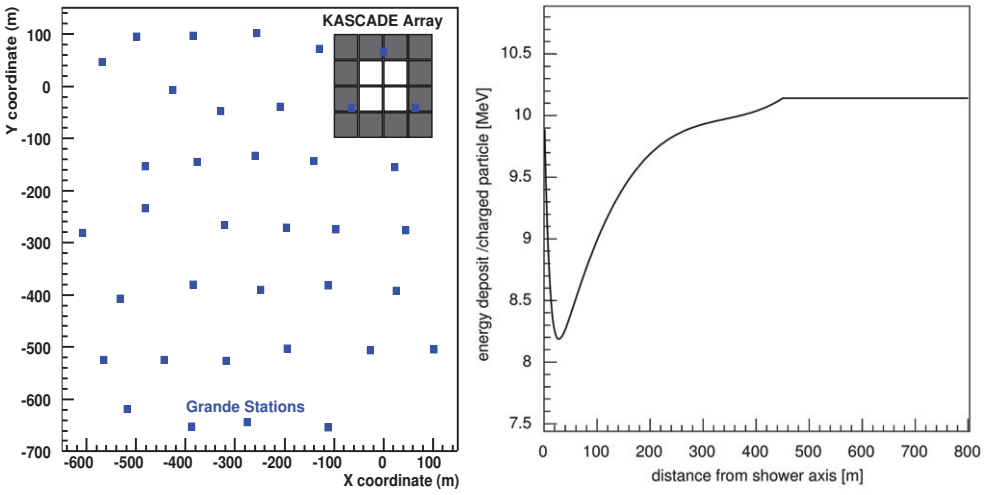

Figure 3. The KASCADE-Grande stations (rectangles) are shown relative to the KASCADE array. The LECF of the Grande stand-alone analysis for the electromagnetic component is shown on the right. Starting at $\sim 300\,\mathrm{m}$ the contribution from muons starts to get dominant. Above $\sim 400\,\mathrm{m}$ only muons contribute to the energy deposit and above 450 m the LECF corresponds to the energy deposited by a single, vertically incident muon. (See [2])

and Raikin [9].

The energy deposits are again transformed into particle densities using LECFs. The LECF for the electromagnetic component is shown in Fig. 3. The shape is mainly governed by the distance-dependent γ/e ratio and the energy distribution of electrons and photons. Unlike for the KASCADE LECF, a dependence on the shower size has been found to be negligible and does not contribute to the LECF.

In step two of the reconstruction procedure, the core position found in step one is moved on a 7×7 grid with a spacing of 8 m. Each position is used as a fixed parameter in the fit of the LDF to the charged particle densities leaving the shape parameter and N_{ch} as the only free parameters. The position resulting in the smallest χ^2 is kept as the fixed core position for the next two steps.

Next, the arrival direction is reconstructed more precisely by fitting the arrival times using a theoretical shower front derived from simulations.

After that the shape parameter and N_{ch} are fitted using again the core position obtained in step two.

The final location of the shower core is reconstructed by fitting the LDF again. This time the core position can vary freely, but N_{ch} and the slope are fixed.

Using this position, the final values for arrival direction, N_{ch} and the slope parameter are derived by repeating the steps three and four.

The number of muons can now be reconstructed by using the core position and arrival direction reconstructed for the Grande detectors and fitting the muon LDF with N_{μ} being again the only free parameter.

3.2. The Energy Spectrum

The analysis is again based on the two-dimensional shower size spectrum, which is shown on the left side in Fig. 4. Due to low statistics and larger uncertainties in N_{ch} and N_{μ} being a problem for the unfolding analysis used for the KASCADE analysis, the first Grande analyses use a different approach to be able to really reach up to 1 EeV.

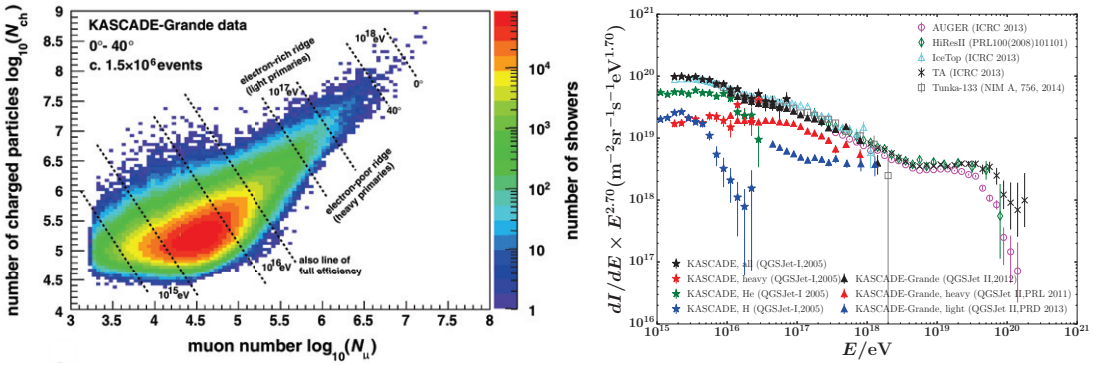

Figure 4. Left: The two-dimensional shower size spectrum derived from Grande data (See [10]). Right: All-particle spectra of several experiments are shown in addition to composition measurements of the KASCADE and KASCADE-Grande arrays.

The reconstruction of the energy is based primarily on N_{ch}, however, the ratio of N_{ch} to N_{μ} as a function of N_{ch} is used to take the mass-dependence of the energy corresponding to a certain number of charged particles into account. As explained in [11], the following formulas are used:

$$\log_{10}(E) = [a_{\mathrm{H}} + (a_{\mathrm{Fe}} - a_{\mathrm{H}}) \cdot k] \cdot \log_{10}(N_{\mathrm{ch}}) + b_{\mathrm{H}} + (b_{\mathrm{Fe}} - b_{\mathrm{H}}) \cdot k \tag{2}$$

with

$$k = \frac{\log_{10}(N_{\mathrm{ch}}/N_{\mu}) - \log_{10}(N_{\mathrm{ch}}/N_{\mu})_{\mathrm{H}}}{\log_{10}(N_{\mathrm{ch}}/N_{\mu})_{\mathrm{Fe}} - \log_{10}(N_{\mathrm{ch}}/N_{\mu})_{\mathrm{H}}} \tag{3}$$

and

$$\log_{10}(N_{\mathrm{ch}}/N_{\mu})_{\mathrm{H,Fe}} = c_{\mathrm{H,Fe}} \cdot \log_{10}(N_{\mathrm{ch}}) + d_{\mathrm{H,Fe}} \tag{4}$$

The coefficients are derived using simulated proton and iron showers. Since the k parameter is mass sensitive, it can be used to separate the events in a light and a heavy mass group. This is done by comparing the measured value of k with the mean, energy-dependent values of k for simulations of showers induced by particles of five different masses. See [10][12] for detailed descriptions of this procedure.

The resulting all-particle spectrum [11] and the spectra for the light [12] and heavy [10] mass groups are shown on the right side of Fig. 4.

The spectrum of heavy primaries shows a knee-like structure at around 80 PeV. This is the energy 26 times higher than the energy where the proton knee was found to be. This indicates a charge dependent position of the knees, however, the true composition of the heavy mass group is not entirely known. We only state that it is heavy, not that it is iron only. Iron dominating the heavy component does make sense from a theoretical point of view, though, and is indicated by the results of an unfolding analysis based on Grande data [13].

The spectrum of light primaries exhibits an ankle-like structure at about 126 PeV. The slope of the spectrum at energies below this feature is almost identical to the slope of the spectrum of heavy primaries above its knee-like structure. Assuming that the heavy galactic component reaches an end, the light component above the ankle-like feature could be considered to be of extragalactic origin. According to the QGSJetII-02 [14] based simulations, the light component should consist mainly of H + He, however, this depends on the hadronic interaction model that is used (See e.g. [15] for a comparison). If one interprets, for example, EPOS [16] simulated data in the light of QGSJetII-02 calibrations, the light component could be a pure proton component. The existence of both features does not depend on the hadronic interaction model used, only

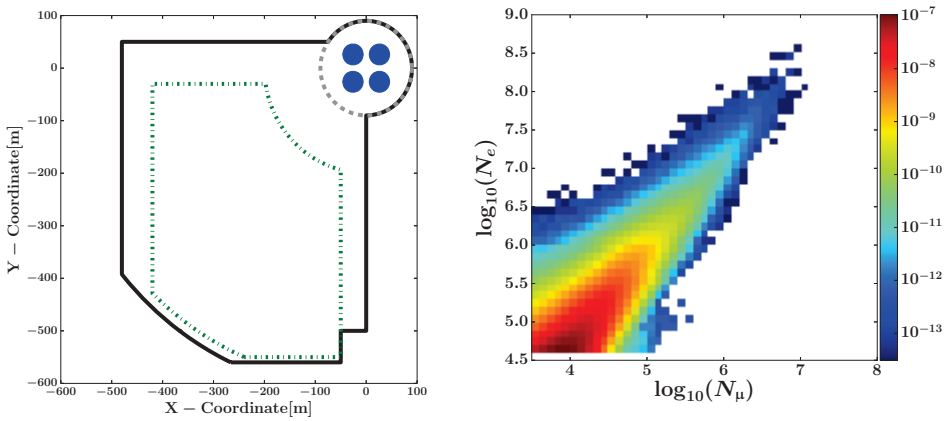

Figure 5. Left: The effective areas for the combined analysis (solid), KASCADE-Grande area (dot-dashed) and KASCADE (dashed) are shown. In addition a possible sub-KASCADE selection for reaching lower energies is shown as full circles. Right: The current two-dimensional shower spectrum of the combined analysis.

the relative fluxes of each component and the exact location of the two features change when using different models.

To improve the knowledge about the composition and to counter the differences between the results for KASCADE and KASCADE-Grande, a combined analysis using the same interaction models and reconstruction procedures is being performed. This new analysis is briefly described in the next section.

4. Combined Analysis

The combined analysis treats the KASCADE and KASCADE-Grande arrays as one single detector. The reconstruction of the shower observables follows the one described in section 2.2 (KASCADE), however, the Grande detectors are now included during the fitting processes. The energy deposits in the detectors are still translated into particle densities using the LECFs described in sections 2.2 and 3.1. Independent LECFs are needed because of the different scintillation detector configurations (thickness of the scintillators, surrounding material etc.).

Especially the events with a core position inside the Grande array and near the KASCADE detectors profit from the additional information provided by the latter, but also the reconstruction of the KASCADE events improve because of the larger distance range that gets available by adding the Grande detectors.

One of the improvements is the increase in the number of events. For KASCADE the increase compared to the stand-alone analysis shown in section 2.3 is based on a larger zenith angle range and, for part of its accessible energy range, a larger fiducial area. For the Grande energy range this is achieved mainly by using a larger fiducial area (left side of Fig. 5). Unfortunately, spanning such a large energy range, as is planned for this analysis, is not possible if the large area is to be used for the entire combined spectrum. Large showers inside or very near to the KASCADE array will result in an overestimation of the number of muons due to high energetic particles passing the shielding. Small showers farther away from the muon detectors will also result in a unreliable reconstruction of the total number of muons. Therefore, the chosen area has to depend on the size of the shower, using the KASCADE array for small showers, the total area for showers of intermediate size and excluding the KASCADE area for large showers. Although there are in total four different areas involved, we do not see significant transition effects in the

two-dimensional shower-size plot, shown on the right side of Fig. 5. This is a good indication that the reconstruction works as expected. There are also plans to use a sub-KASCADE selection, shown as four full circles in Fig. 5, to try to get further down in energy towards 10^{14} eV, but this possibility is still under investigation.

5. Conclusion

The reconstruction procedure of the KASCADE array has been fully adapted to the combined use of both, the KASCADE and KASCADE-Grande detectors. The current state of the analysis is already a good basis for the final reconstruction of the energy spectrum and the determination of the mass composition in the energy range from 10^{15} (10^{14}) to 10^{18} eV. However, a lot of cross-checks on the area (energy) dependent reconstruction uncertainties are still to be done and an optimization for a reconstruction of lower energetic showers using sub-KASCADE area selections, as indicated by the full circles in Fig. 5, is also foreseen.

Acknowledgment

The authors would like to thank the members of the engineering and technical staff of the KASCADE-Grande collaboration, who contributed to the success of the experiment. The KASCADE-Grande experiment is supported in Germany by the BMBF and by the Helmholtz Alliance for Astroparticle Physics - HAP funded by the Initiative and Networking Fund of the Helmholtz Association, by the MIUR and INAF of Italy, the Polish Ministry of Science and Higher Education, and the Romanian Authority for Scientific Research UEFISCDI (PNII-IDEI grants 271/2011 and 17/2011).

References

[1] Antoni T *et al.* 2003 *Nucl. Instrum. Methods Phys. Res., Sect. A* **513** 490–510 ISSN 0168-9002

[2] Apel W *et al.* 2010 *Nucl. Instrum. Methods Phys. Res., Sect. A* **620** 202–216 ISSN 0168-9002

[3] Apel W *et al.* 2006 *Astropart. Phys.* **24** 467–483

[4] Kamata K and Nishimura J 1958 *Prog. Theor. Phys. Suppl.* **6** 93–155

[5] Greisen K 1960 *Ann. Rev. Nucl. Sci.* **10** 63–108

[6] Antoni T *et al.* 2005 *Astropart. Phys.* **24** 1–25 ISSN 0927-6505

[7] Kalmykov NN O S and AI P 1997 *Nucl. Phys. B (Proc. Suppl.)* **52** 17–28

[8] Engel R 1999 *International Cosmic Ray Conference* (*International Cosmic Ray Conference* vol 1) p 415

[9] AA L and RI R 2001 *Nucl. Phys. Proc. Suppl.* **97** 274

[10] Apel W D *et al.* (KASCADE-Grande Collaboration) 2011 *Phys. Rev. Lett.* **107**(17) 171104

[11] Apel W *et al.* 2012 *Astropart. Phys.* **36** 183 – 194 ISSN 0927-6505

[12] Apel W *et al.* 2013 *Phys. Rev. D* **87**

[13] Apel W *et al.* 2013 *Astropart. Phys.* **47** 54–66

[14] Ostapchenko S 2006 *Nucl. Phys. B, Proc. Suppl.* **151** 143 – 146 ISSN 0920-5632

[15] Apel W *et al.* 2014 *Adv. Space Res.* **53** 1456–1469

[16] Pierog T and Werner K 2009 *Nucl. Phys. B, Proc. Suppl.* **196** 102 – 105 ISSN 0920-5632 10.1016/j.nuclphysbps.2009.09.017